Journal of Marine Science and Technology

Volume 25 | Issue 6 Article 12

REAL-TIME METHOD FOR CALCULATING RETARDATION FUNCTIONS

Li-hao Yuan
College of Shipbuilding Engineering, Harbin Engineering University, Harbin, Heilongjiang, China.

Yue-sheng Ma
College of Shipbuilding Engineering, Harbin Engineering University, Harbin, Heilongjiang, China.

Ying-fei Zan
College of Shipbuilding Engineering, Harbin Engineering University, Harbin, Heilongjiang, China.,
zanyingfei@hrbeu.edu.cn

Zhao-hui Wu
Offshore Oil Engineering Co., Ltd., Tianjin, China.

Recommended Citation

Yuan, Li-hao; Ma, Yue-sheng; Zan, Ying-fei; and Wu, Zhao-hui (2017) "REAL-TIME METHOD FOR CALCULATING RETARDATION FUNCTIONS," *Journal of Marine Science and Technology*: Vol. 25: Iss. 6, Article 12.
DOI: 10.6119/JMST-017-1226-12
Available at: https://jmstt.ntou.edu.tw/journal/vol25/iss6/12

REAL-TIME METHOD FOR CALCULATING RETARDATION FUNCTIONS

Acknowledgements

The authors are grateful to the Fundamental Research Funds for the Central Universities (HEUCFJ170103) and the Marine Engineering Equipment Scientific Research Project of Ministry of Industry and Information Technology of PRC.

Journal of Marine Science and Technology, Vol. 25, No. 6, pp. 715-721 (2017)
DOI: 10.6119/JMST-017-1226-12

REAL-TIME METHOD FOR CALCULATING RETARDATION FUNCTIONS

Li-hao Yuan[1], Yue-sheng Ma[1], Ying-fei Zan[1], and Zhao-hui Wu[2]

Key words: state-space model, retardation functions, roll decay test, real-time calculation.

ABSTRACT

To meet the demand for real-time calculation of time-domain motion equations, a state-space model was established to replace the convolution integral method to improve computational efficiency. On the basis of the HYSY201 vessel, the impulse response curve fitting method and the realization theory method based on the time-domain identification theory were compared to establish the state-space model. The results of roll decay simulation conducted using the state-space model and the convolution integral method were verified against decay test results. The simulation results for retardation function, radiation forces, and motion time histories calculated using the state-space model and the convolution integral method were compared and analyzed. The roll decay simulation results agreed with the model experiment results. The simulation results demonstrated that the retardation function, radiation forces, and motion time histories calculated using the state-space model agreed adequately with those calculated using the convolution integral method. Moreover, the simulation based on the state-space model ran approximately 28 times faster than that based on the convolution integral method. Thus, replacing the convolution integral method with the state-space model improves computational efficiency, while maintaining calculation accuracy.

I. INTRODUCTION

The frequency-domain method has been applied for seakeeping analysis since before the time-domain method; for example, Du et al. (2011) applied this method to calculate the hydrodynamic coefficient. However, with the rapid development of the offshore oil industry worldwide, marine operations are moving toward deeper waters, and nonlinear problems are involved as well. Many of the actual conditions of a vessel cannot be explained using the traditional frequency-domain method. Because of the fundamental limitation of the frequency-domain method, it is suitable only for treating steady-state problems, and it cannot be used to solve nonlinear and transient problems. Therefore, the time-domain method was applied by Hu et al. (2017) to treat nonlinear dynamics and impact load during float-over installation.

The time-domain method had first been proposed by Cummins (1962) and Ogilvie (1964), who used a retardation function with a convolution term to represent the memory effects of a fluid. Suresh and Nuno (2015) investigated how a nonlinear term influences calculations of ship motion response. Sen (2002) applied a time-domain method to calculate large-amplitude three-dimensional ship motions with forward speed. Chen et al. (2014) analyzed time-domain modeling of a dynamic impact oscillator under wave excitations. Chang et al. (2008) employed the frequency-time-domain transform method (FTTM) to calculate the rolling motion time histories of surface ships. Frequency-domain hydrodynamic coefficients were converted by Bao and Kinoshita (1992) by using the fast Fourier transform method instead of the direct time-domain method. Compared with the direct time-domain method, the FTTM has the advantage of quick and simple calculation. Because high-frequency damping coefficients are not included, the calculation results are not accurate. Bao and Kinoshita (1992) proposed an asymptotic solution of wave-radiating damping at high frequencies. Tang et al. (2013) and Tang et al. (2014) have applied the frequency-time-domain method to calculate the retardation function of the time domain by analyzing the motion of a body floating on waves. The use of a damping correction method to add the high-frequency damping coefficients could greatly improve the calculation accuracy, but the errors caused by this correction have not been investigated, and the results obtained using the method have not been validated by performing a model experiment. Yu and Falnes (1998) used the state-space model (SSM) to simulate the heaving motion of a cylindrical riser in marine engineering. Perez and Fossen (2011) applied the frequency-domain identification method to study dynamic models of marine structures by using hydrodynamic data. The results showed that computational efficiency increased considerably. However, an in-depth investigation that considers the effect of the respective degrees of freedom has not been conducted.

To realize the strategic goal of exploitation of oil and natural

Paper submitted 09/14/17; revised 10/24/17; accepted 11/09/17. Author for correspondence: Ying-fei Zan (e-mail: zanyingfei@hrbeu.edu.cn).
[1] College of Shipbuilding Engineering, Harbin Engineering University, Harbin, Heilongjiang, China.
[2] Offshore Oil Engineering Co., Ltd., Tianjin, China.

gas from shallow waters to deep sea, real-time prediction and safety assessment of marine engineering operations such as offshore pipeline installation, float-over installation, and floating crane are carried out in the harsh marine environment of the South China Sea. The time-domain motion model contains a convolution term, which is not efficient from the viewpoint of numerical calculation and not convenient for analysis and design of motion control systems (Fossen, 2002). Therefore, by using the HYSY201 vessel as the object of study, which could conduct pipeline installation operations at depths of 3,000 m, this study performed a theoretical real-time simulation of marine engineering operations.

In the present study, two time-domain identification methods were used to establish the state-space model (SSM) to replace the convolution integral method (CIM). The roll decay simulation results were verified against experimental data, and the verification results indicated that the numerical method is adequately accurate and provides a reliable theoretical reference for marine operations. Compared with the CIM, the simulation results for retardation functions, radiation forces, and motion time histories calculated using the SSM agreed adequately with each other; moreover, computational efficiency was improved considerably, which proves that this method can fulfill the requirement of real-time computation. Furthermore, it can be used in many practical marine engineering applications such as real-time decision-making, offshore pipeline installation, floating crane training simulators, and motion prediction systems.

II. TIME-DOMAIN ANALYSIS METHOD

Starting from Newton's second law and assuming that the vessel oscillates slightly, Cummins (1962) established the following sea-keeping equation in the time domain:

$$(m + A_\infty)\ddot{\xi} + D\dot{\xi} + \int_0^t K(t-\tau)\dot{\xi}(\tau)d\tau + G\xi = F_{wave}^{exc} \tag{1}$$

where A_∞ represents the infinite-frequency added mass. $A(\omega)$ and $D(\omega)$ indicate the frequency-dependent added mass and damping coefficient, respectively. $G(\eta)$ and F_{wave}^{exc} represent the hydrostatic matrix and wave-excitation force, respectively. $K(t)$, which is important for calculating the time-domain equation, is called the retardation function and is a result of the memory effects of the fluid.

Eq. (1) contains the convolution term, the calculation of which is very time consuming during simulation. Therefore, to increase the efficiency of computing the free-surface memory effects, Kristiansen et al. (2006) proposed that the CIM can be replaced by the linear SSM

$$u = \int_0^\infty K(t)\dot{\xi}(\tau)d\tau \cong \begin{cases} \dot{x}_r = A_r + B_r\dot{\xi} \\ u = C_r\xi_r \end{cases} \tag{2}$$

where ξ is the state vector; A_r, B_r, and C_r represent the constant coefficient matrices of the SSM.

The advantage of the state-space model is that any future state of the system depends only on the present value of the system state vector ξ. In other words, no past information needs to be stored as in the case of the convolution method, because the memory effect is contained in its entirety in the state vector.

The hydrodynamic software WAMIT was used to solve the frequency-dependent added mass and damping coefficient of the low- to high-frequency fluid. The SSM can be obtained using time-domain identification methods based on the frequency-dependent damping coefficient.

The hydrodynamic coefficients and the retardation function were established by Ogilvie (1964):

$$\begin{aligned} A(\omega) &= A_\infty - \frac{1}{\omega}\int_0^\infty K(t)\sin(\omega t)dt \\ D(\omega) &= \int_0^\infty K(t)\cos(\omega t)dt \end{aligned} \tag{3}$$

Taking the inverse Fourier transform of Eq. (3) yields the retardation function $K(t)$ as follows:

$$K(t) = \frac{2}{\pi}\int_0^\infty D(\omega)\cos(\omega t)d\omega \tag{4}$$

The retardation function $K(t)$ has the following properties:

(1) The low-frequency asymptotic value is given by $\lim_{t\to 0} K(t) = \frac{2}{\pi}\int_0^\infty D(\omega)\cos(\omega t)d\omega \neq 0 < \infty$

(2) The high-frequency asymptotic value is given by $\lim_{t\to \infty} K(t) = \frac{2}{\pi}\int_0^\infty D(\omega)\cos(\omega t)d\omega = 0$

III. SSM ESTABLISHMENT

A good SSM should have the following properties:

(1) It must satisfy the properties of the retardation function.
(2) It must be stable.
(3) It must be convenient from the viewpoint of applying identification methods.

According to the preceding conditions, the solution of the SSM is simplified to find the optimal solution by least-squares fitting:

$$K_{kj}(\mathrm{j}\omega) \approx \hat{K}_{kj}(s = \mathrm{j}\omega) \tag{5}$$

where $\hat{K}_{kj}(s)$ is the retardation function to be obtained, and it is expressed as follows:

$$\hat{K}_{kj}(s,\theta)=\frac{P_{kj}(s,\theta)}{Q_{kj}(s,\theta)}=\frac{p_m s^m+p_{m-1}s^{m-1}+\cdots+p_0}{s^n+q_{n-1}s^{n-1}+\cdots+q_0} \tag{6}$$

where $\theta=[p_m,\ldots p_0,q_{n-1},\ldots q_0]$ is defined as a parameter vector, which is converted into a curve fitting problem.

According to the properties of the retardation function, the SSM must satisfy the following characteristics:

(1) $\hat{K}_{kj}(0)=0$.
(2) Characteristic matrix of the SSM is full rank.
(3) SSM is stable.
(4) $\hat{K}_{kj}(s)$ is positive real.

According to the properties of the retardation function, the SSM is established using identification theory. The fitting quality of the SSM is evaluated by the confidence parameter R^2, which is expressed as follows:

$$R^2=1-\frac{\sum(K_{kj}-\tilde{K}_{kj})^2}{\sum(K_{kj}-\bar{K}_{kj})^2} \qquad 0\le R^2\le 1 \tag{7}$$

where K_{kj} is the expected value of the retardation function, $\tilde{K}_{kj}$ is the fitting value of the retardation function, and $\bar{K}_{kj}$ is the expected average value of the retardation function. The closer the value is to 1, the better is the quality of the fit.

IV. TWO IDENTIFICATION METHODS

The SSM can be established on the impulse response of the retardation function. The conversion of the frequency domain to the time domain induces an additional error, which can be minimized depending on the manner in which $K(\omega)$ is translated into $K(t)$.

$$K_{kj}(t)=IFFT\left(K_{kj}(\omega)\right) \tag{8}$$

However, this method is limited by the frequency range because the hydrodynamic software calculates only over a finite frequency range, and the retardation function $K_{kj}(t)$ will eventually be calculated by the mean interval from 0 to the maximum value of t, which may lead to a drastic change in the impulse response function for small values of t. Alternatively, the trapezoidal integral method can be used to calculate the retardation function:

$$\begin{aligned}K_{kj}(t)=&\frac{\Delta\omega}{\pi}\sum_{k=1}^{k_{\max}-1}2B_{kj}(k\Delta\omega)\cos(k\Delta\omega t)\cdots\\&+\frac{\Delta\omega}{\pi}(B_{kj}(0)+B_{kj}(k_{\max})\cos(k_{\max}\Delta\omega t)\end{aligned} \tag{9}$$

1. Impulse Response Curve Fitting Method

The impulse response curve fitting method (IRCFM) obtains the corresponding impulse response function based on the z-transform proposed by Lin (1982), and the function returns the coefficients of the numerator and denominator of the discrete rational system. The expression is as follows:

$$H(z)=\frac{\sum_{k=0}^{q}b[k]z^{-k}}{1+\sum_{l=0}^{p}a[l]z^{-l}} \tag{10}$$

where b and a are the vector numerator coefficients and denominator coefficients, respectively, of Eq. (10). After all denominator and numerator coefficients are obtained, the transfer function H(z) can be obtained. However, for a complex high-order equation, this method cannot guarantee the stability of the SSM.

2. Realization Theory Method

In the realization theory method (RTM), an identification method based on singular value decomposition was applied by Wang (2015) to obtain the impulse response function. The calculations in the RTM are easier when applied to a discrete-time system than when applied to a continuous-time system. Thus, the RTM calculations are first performed in indiscrete time. Once the parameters of the discrete-time system are obtained, the RTM can apply bilinear transformation to convert the model into a continuous-time system. Taghipour et al. (2008) applied bilinear transformation to guarantee the stability of the continuous-time system. The impulse response function can be solved to output the equivalent SSM matrices $\bar{A}_r$, $\bar{B}_r$, $\bar{C}_r$, and $\bar{D}_r$:

$$A_r=\bar{A}_r,\ B_r=\bar{B}_r,\ C_r=\bar{C}_r\Delta t,\ D_r=\bar{D}_r\cdot 0=0 \tag{11}$$

The matrix $\bar{D}_r$ is constrained to a value of 0 to maintain the causal relationship of the system. The equation of state can produce a very accurate fitting model ($R^2\ge 0.99$), but the order used ($i\ge 200$) is very high. In fact, this equation can be approximated as a second-order system ($R^2>0.98$). A lower-order system is obtained using the reduced-order method, order of the SSM is reduced to the second order, and then the order of the system is increased until a high-quality effect is obtained.

The principal parameters of the HYSY201 vessel are listed in Table 1.

Two time-domain identification methods were applied in this study to fit the retardation function in the time domain. The confidence parameter was set to 0.99. In this section, three degrees of freedom, namely surge, heave, and pitch, are considered.

Table1. Principal vessel dimensions.

Parameter	Symbol	Unit	Value
Length overall	LOA	m	204.65
Length between Perpendiculars	LPP	m	185.00
Breadth moulded	B	m	39.20
Breadth depth	D	m	14.00
Draught	d	m	8.959
Displacement	Δ	t	55101.80

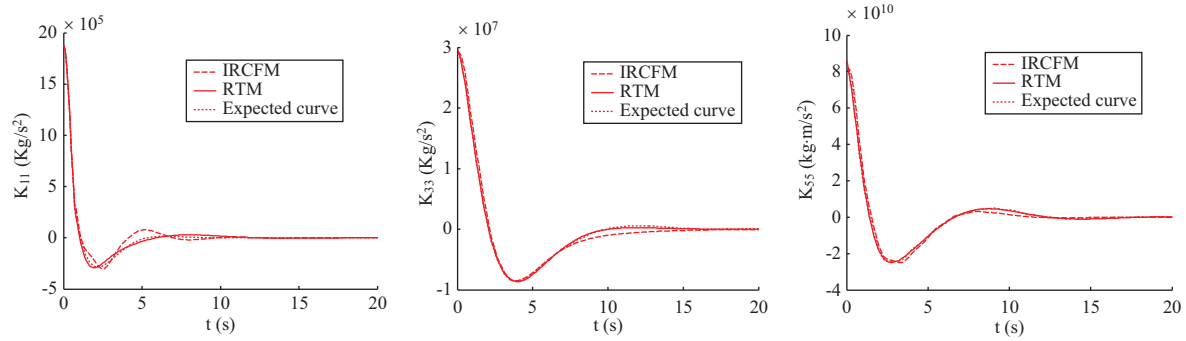

(a) Surge retardation function fitted with two time-domain methods (b) Heave retardation function fitted using two time-domain methods (c) Pitch retardation function fitted using two time-domain methods

Fig. 1. Comparison of retardation functions fitted using different time-domain identification methods.

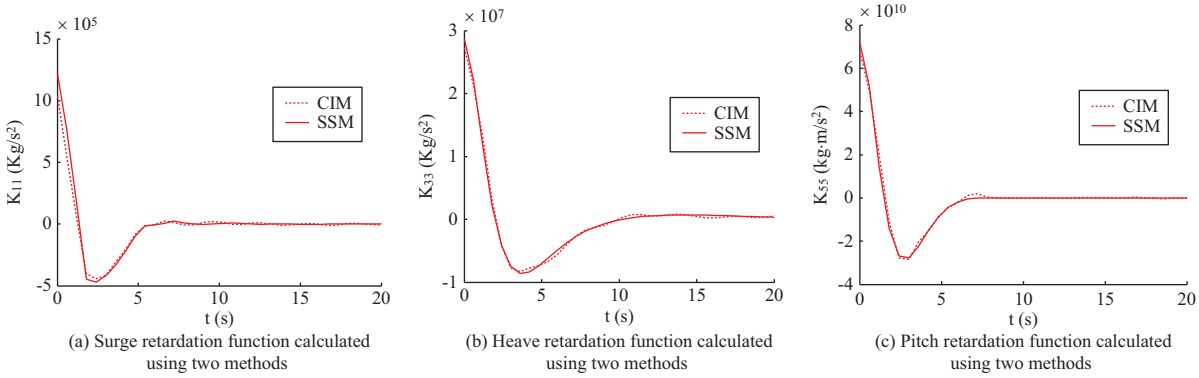

(a) Surge retardation function calculated using two methods (b) Heave retardation function calculated using two methods (c) Pitch retardation function calculated using two methods

Fig. 2. Comparison of retardation functions calculated using CIM and SSM.

The retardation functions fitted using the IRCFM and RTM are shown in Fig. 1.

Fig. 1 shows comparisons of the retardation functions fitted using the two time-domain methods:

(1) Considering the degree of freedom pitch, the retardation function curves of the time-domain IRCFM and RTM were generally consistent with the expected curve. However, considering the degrees of freedom surge and heave, the IRCFM had a worse quality of fit than the RTM, and this is because the damping curve of the IRCFM has a slight mutation, which indicates that the IRCFM is more susceptible to curve smoothness.

(2) When the confidence parameter was kept consistent, the fitting result obtained using the RTM was more consistent with the expected value of the retardation function than the fitting result obtained using the IRCFM, which implies that the RTM yields a better fit and is more suitable for fitting the curve of the retardation function.

Therefore, the RTM based on time-domain identification theory was applied to establish the SSM.

V. COMPARISON OF RETARDATION FUNCTIONS OBTAINED USING SSM AND CIM

Based on the comparison of the two time-domain identification methods in the preceding section, the SSM was established

Fig. 3. Roll decay test of HYSY201 vessel model.

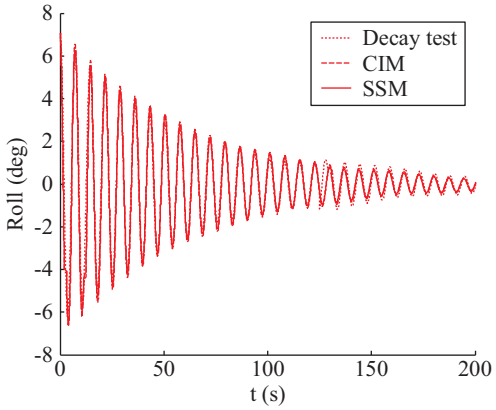

Fig. 4. Verification of results calculated using CIM, SSM, and decay test.

using the RTM and compared with the numerical CIM from the viewpoint of calculating the retardation function. Time stepping was controlled using the parameter time step, and its default value was set to 0.01 s. As shown in Fig. 2, the retardation functions of the three degrees of freedom, namely surge, heave, and pitch, were calculated using the SSM and CIM.

Fig. 2 shows a comparison of the retardation functions calculated using the CIM and SSM:

(1) The retardation functions calculated using the CIM and SSM were generally consistent with each other. The retardation function was first decreased to the minimum value; then, it increased gradually and finally became zero. This proves that the SSM is accurate and can replace the CIM for calculating the retardation function.
(2) Compared with the retardation function of surge, the retardation functions of heave and pitch calculated using the SSM were more consistent with the functions calculated using the CIM, which is partly because the radiation damping curve of surge calculated using WAMIT shows a slight mutation.

VI. VERIFICATION OF NUMERICAL CALCULATION AGAINST DECAY TEST RESULTS

A roll decay test was performed in the wave-resistant wave pool at the China Vessel Science Research Center by using a scaling factor of 1:48.684. Specifically, under the hydrostatic condition, a roll moment was exerted on the side of the vessel model to induce rolling motion of the model, and roll time histories were recorded in real time on a computer hard disk. The roll inherent period of the HYSY201 vessel under the 4000-t prelifting condition was 17.1 s, as obtained by analyzing roll decay curve data. A photograph of the roll decay test in still water is shown in Fig. 3.

The conditions in this study were consistent with selected model test conditions, to ensure the reliability of the contrast results. Time stepping in the two numerical methods was controlled using the parameter time step, which was set to 0.01 s by default. Contrast curves calculated using the CIM, SSM, and decay test are plotted in Fig. 4.

From the comparison of the results calculated using the CIM, SSM, and decay test in Fig. 4, it could be concluded that the results calculated using CIM and SSM were moistly consistent with those obtained from the decay test, especially before the suitable time of 120 s. The slight difference between the results obtained using CIM, SSM, and the decay test may be attributed to the potential damping coefficient based on WAMIT when the decay results were very small after 120 s. In addition, for such a free decay test of 200 s, the simulation time of the SSM was 6.86 s; however, the simulation time of the CIM was 30 s. Therefore, the SSM reduced the simulation time by a factor of 3.24. Thus, the SSM could yield accurate and reliable results efficiently.

VII. COMPARISON OF SIMULATION RESULTS OF THE SSM AND CIM

1. Comparison of Radiation Forces of SSM and CIM

Based on results of the retardation function, radiation force results of surge, heave, and pitch were calculated using the SSM and CIM. The significant wave height and peak period of the Bretschneider spectrum were set to 2.5 m and 8 s, respectively, to calculate wave excitation forces. The wave direction was set to zero and along the bow. The initial conditions of the radiation forces were set to zero. The radiation force results of the three degrees of freedom surge, heave, and pitch are plotted in Fig. 5.

The results obtained from the analysis of the radiation forces calculated using the CIM and SSM are shown in Fig. 5:

(1) The radiation forces of the three degrees of freedom surge, heave, and pitch, calculated using the CIM and SSM, were consistent with each other after the suitable time of 65 s, which indicates that the SSM can replace the CIM for calculating radiation forces.
(2) The radiation forces of the three degrees of freedom were mostly inconsistent with each other before 65 s, which is

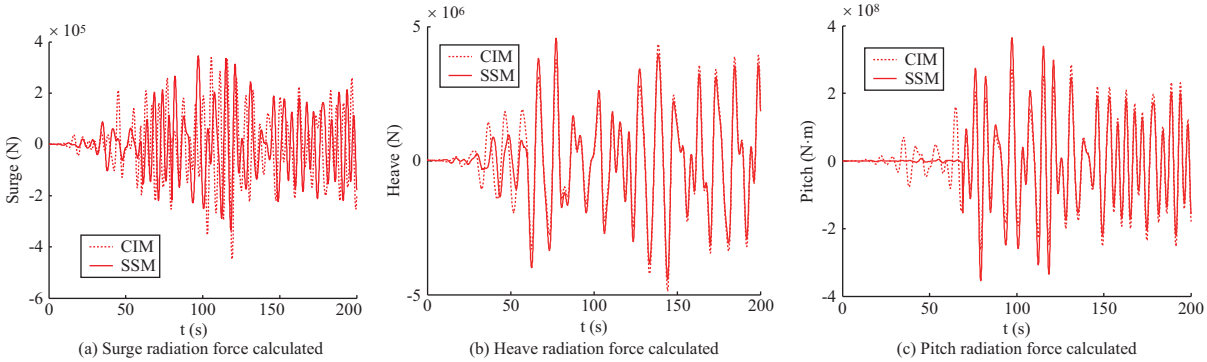

(a) Surge radiation force calculated using two methods (b) Heave radiation force calculated using two methods (c) Pitch radiation force calculated using two methods

Fig. 5. Comparison results of radiation forces calculated using CIM and SSM.

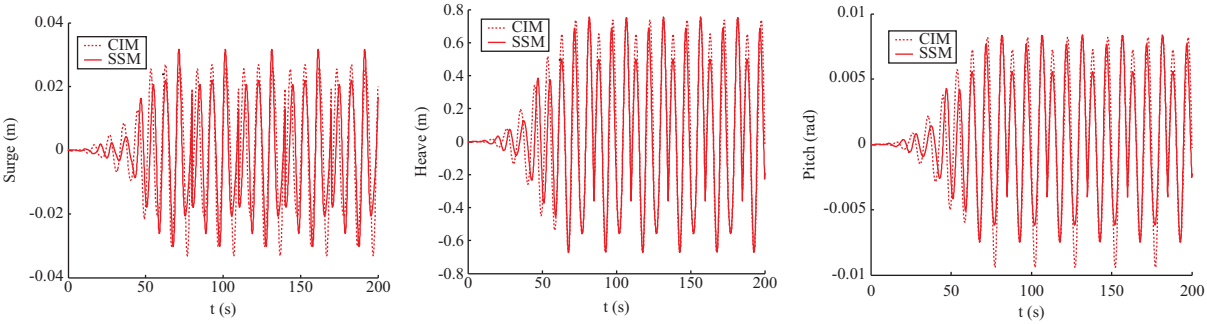

(a) Surge motion time histories calculated using two methods (b) Heave motion time histories calculated using two methods (c) Pitch motion time histories calculated using two methods

Fig. 6. Comparison of motion time histories calculated using CIM and SSM.

because of the difference in dealing with the memory effects of the CIM and SSM.

(3) Compared with the radiation forces of surge, those of heave and pitch were more consistent between the CIM and SSM owing to the good fitting results of the retardation functions.

2. Comparison of Motion Time Histories of SSM and CIM

Based on the time-domain motion equation, Eq. (1), motion time histories of surge, heave, and pitch are plotted in Fig. 6, as derived using the SSM and CIM. The initial conditions for motion response were set to zero, consistent with the condition under which the radiation forces were calculated.

The motion time histories calculated using the CIM and SSM are plotted in Fig. 6 for comparison:

(1) The motion time histories of the three degrees of freedom surge, heave, and pitch, calculated using the SSM, were consistent with those calculated using the CIM, indicating that the SSM can replace the CIM for predicting motion time histories.

(2) The motion time histories of the three degrees of freedom calculated using the two methods were mostly inconsistent with each other before 65 s, which may be ascribed to the calculated radiation forces.

In addition, the time required for time-domain simulation using the CIM to calculate motion time histories was 10.26 min; however, for the SSM, the required time was only 22.36 s, indicating that the SSM shortened the simulation time by a factor of 28. Thus, the SSM has higher computational efficiency and is more suitable for time-domain simulation.

VIII. CONCLUSION

On the basis of the HYSY201 vessel, this study applied the hydrodynamic software WAMIT to calculate added mass and damping coefficient from low frequency to high frequency. The two time-domain identification methods were analyzed and compared to establish an SSM that can replace the CIM for calculating the retardation function, radiation forces, and motion time histories. The simulation results of roll decay were verified against the results of the model experiment. Key conclusions are presented as follows:

(1) The roll decay simulation results calculated using the SSM and CIM were verified against the results of the decay test. That these results were generally consistent with each other, proving that the numerical calculation methods presented in this paper are convincing.

(2) A comparison of the retardation functions of three degrees

of freedom, namely surge, heave, and pitch, calculated using the SSM and CIM revealed that the SSM is sufficiently accurate and can be used instead of the CIM.

(3) The radiation forces calculated using the SSM and CIM were consistent with each other after the suitable time of 65 s, which indicates that the SSM can be used instead of the CIM to calculate radiation forces

(4) The results of motion time histories calculated using the SSM were consistent with those calculated using the CIM after the suitable time of 65 s. SSM improved the computation efficiency by a factor of 28, which demonstrates that it can be used for real-time calculation.

Therefore, the presented SSM is adequately accurate and more efficient for simulation, satisfies real-time requirements, and is practical for use in marine engineering simulations.

ACKNOWLEDGEMENTS

The authors are grateful to the Fundamental Research Funds for the Central Universities (HEUCFJ170103) and the Marine Engineering Equipment Scientific Research Project of Ministry of Industry and Information Technology of PRC.

REFERENCES

Bao, W. and T. Kinoshita (1992). Asymptotic solution of wave-radiating damping at high frequency. Applied Ocean Research 14(3), 165-173.

Chang, Y., J. Fan and R.-C. Zhu (2008). Analysis of ship parametric rolling in head sea. Journal of Hydrodynamics Ser A 23(2), 204-211. (in Chinese)

Chen, M., E. T. Rodney and S. C. Too (2014). Time domain modeling of a dynamic impact oscillator under wave excitations. Ocean Engineering 76, 40-51.

Cummins, W. E. (1962). The impulse response function and ship motions. Schiffstechnik 9, 101-109.

Du, S. X., D. A. Hudson, W. G. Price and P. Temarel (2011). The occurrence of irregular frequencies in forward speed ship seakeeping numerical calculations. Ocean Engineering 38(1), 235-247.

Fossen, T. I. (2002). Marine Control System: Guidance, Navigation and Controls of Ships, Rigs and Underwater Vehicles. Marine Cybernetics, Trondheim.

Hu, Z. H., X. Li and W. H. Zhao (2017). Nonlinear dynamics and impact load in the float-over installation. Applied Ocean Research 65, 60-78.

Kristiansen, E., A. Hjulstad and O. Egeland (2006). State-space representation of radiation forces in time-domain vessel models. Ocean Engineering 27(1), 2195-2216.

Lin, P. L. (1982). Reduction of transfer functions from the stability-equation method and complex curve fitting. Journal of the Franklin Institute 314(2), 109-121.

Ogilvie, T. F. (1964). Recent progress toward the understanding and prediction of ship motions. Proc. 5th Symposium on Naval Hydrodynamics, Bergen, Norway, 3-80.

Perez T. and T. I. Fossen (2011). Practical aspects of frequency-domain identification of dynamic models of marine structures from hydrodynamic data. Ocean Engineering 38(2-3), 426-435.

Sen, D. (2002). Time-domain computation of large amplitude 3D ship motions with forward speed. Ocean Engineering 29(8), 973-1002.

Suresh, R. and F. Nuno (2015). Simplified body nonlinear time domain calculation of vertical ship motions and wave loads in large amplitude waves. Ocean Engineering 107(1), 157-177.

Taghipour, R., T. Perez and T. Moan (2008). Hybrid frequency-time domain models for dynamic response analysis of marine structures. Ocean Engineering 35(7), 685-705.

Tang, K., R. Zhu and G. Miao (2014). Retard function and ship motions with forward speed in time-domain. Journal of Hydrodynamics 26(5), 689-696.

Tang, K., R.-C. Zhu, G.-P. Miao and J. Fan (2013). Calculation of retard function for time-domain analyzing floating body in waves. Journal of Shanghai Jiao Tong University 47(2), 300-306. (in Chinese)

Wang, Y. G. (2015). Robust frequency-domain identification of parametric radiation force models for a floating wind turbine. Ocean Engineering 109, 580-594.

Yu, Z. and J. Falnes (1998) State-space modelling of dynamic systems in ocean engineering. Journal of Hydrodynamics 24(1), 1-17.